The Effect of Vibrationally Excited Levels on the Pressure Saturation of the Collisional Quenching of the $^3B_1$ State of SO_2

S. C. Bae, S. R. Lee, and J. K. Ku

Department of Chemistry, Pohang University of Science and Technology, Pohang, Kyung-buk 790-784, Korea
Received September 30, 1995

The pressure saturation effect on the phosphorescence decay rates of the $^3B_1$ state of SO_2 has been reinvestigated by the laser induced phosphorescence method in pure SO_2. We have attempted to fit the pressure dependence of the phosphorescence decay rates using the radiationless transition model by introducing different coupling constants for each vibrational level of the $^3B_1$ state. The experimental decay rates can be fitted well, when the coupling constants for the (0,0,0), (0,1,0) and (0,2,0) levels of the $^3B_1$ state are 7.2×10^{-4}, 2.2×10^{-3} and 5.9×10^{-3} cm^{-1}, respectively.

Introduction

The $^3B_1$ state of SO_2 has been extensively studied by several research groups because it is of interest not only to understand its intrinsic molecular properties, but also its practical role in the atmospheric photochemistry.[1~3] The $^3B_1$ state located about 25,700 cm^{-1} above the ground state has an extremely long radiative lifetime and relatively small quenching rate constants. The deactivation of the $^3B_1$ state in SO_2 has been represented by the following three processes.[4~6]

$$^3SO_2 \xrightarrow{k_p} SO_2 + h\nu_p \quad (1)$$

$$^3SO_2 + SO_2 \xrightarrow{k_q} 2SO_2 \quad (2)$$

$$^3SO_2 + SO_2 \xrightarrow{k_c} SO_3 + SO \quad (3)$$

The unimolecular nonradiative decay is ignored because the phosphorescence quantum yield for Eq. (1) was found to be 0.95 ± 0.29 at zero pressure.[7]

Strickler and Rudolph[5] prepared the $^3B_1$ state of SO_2 by collisional relaxation of higher-lying singlet vibronic states which were generated by exciting the ground state molecules with the nitrogen emission line at 315.6 nm, and studied the pressure dependence of the decay rates of the $^3B_1$ state of SO_2 up to 1,400 Torr. They found that the decay rates of the $^3B_1$ state at high pressures are much slower than those expected from the extrapolation of the low pressure data. It was found that the decay rates could be fitted well by the following empirical formula,

$$\frac{1}{\tau} = \frac{1}{\tau^0} + k_c[SO_2] + \frac{k_q[SO_2]}{1+\alpha k_q[SO_2]} \quad (4)$$

where τ^0 is the radiative lifetime of the $^3B_1$ state of SO_2, α is a constant, and k_c and k_q represent chemical and physical quenching rate constants, respectively. Eq. (4) clearly shows that the physical quenching process, Eq. (2), is saturated at high pressures since the last term on the right-hand side of the Eq. (4) is reduced to a constant ($1/\alpha$) at high pressures. Strickler and Rudolph[5] proposed two models, the kinetic and the radiationless transition models, to explain this pressure saturation of the phosphorescence decay rates of the $^3B_1$ state of SO_2, and they found that the experimental data were better fitted with the kinetic model. The kinetic model, however, is not appropriate to explain the pressure saturation effect (see section III B).

Strickler and Ito[6] investigated the temperature dependence of the pressure saturation effects as well as the phosphorescence spectra. They observed strong temperature dependence of the limiting decay rates at high pressures, but the phosphorescence spectra showed emissions only from the $a^3B_1 \rightarrow X^1A_1$ transition. They found that the results from the temperature dependence experiments could also be rationalized by both models. Nevertheless, the absence of any fluorescence or phosphorescence emissions other than the $a^3B_1 \rightarrow X^1A_1$ transition favored the radiationless transition model even though the fitting of the experimental data was not so good.

In this work, we have prepared directly the $^3B_1$ state of SO_2 molecules by laser excitation of the $^3B_1(0,0,0)$ level from the ground state molecules at 388.3 nm, and reinvestigated the pressure saturation of the phosphorescence decay rates. It is found that the experimental decay rates can be fitted well using the radiationless transition model of Strickler and Rudolph[5] when different values of the coupling matrix element β are used for the vibrationally excited levels of the $^3B_1$ state. We have also investigated the phosphorescence spectra in the 400-800 nm range, but no evidence for extra emissions other than the $a^3B_1 \rightarrow X^1A_1$ transition was detected.

Experimental Setup

Details of the experimental setup were reported in elsewhere.[8] The phosphorescence cell was made of a 2 l (radius=7.8 cm) Pyrex bulb, and two pairs of 1 inch Pyrex O-ring joints were attached for the windows of the laser beam path and for the connection of the cell to a gas handling vacuum rack. The phosphorescence was collected through a 1.5 inch observation window attached to the bulb with a short (<1.5 cm) arm. The SO_2 gas was purchased from Matheson and purified by the freeze and thaw method before storing in a storage bulb. The pressures in the cell were measured with an oil manometer at low pressures, but a mercury manometer was used for the pressures above 40 Torr. The Nd : YAG pumped dye laser (Quantel YG681-TDL 60) with 8 ns pulse width was tuned at 388.3 nm to populate the $^3B_1(0,0,0)$ level of SO_2. The phosphorescence time profiles from the $^3B_1$ state were monitored at 90° from the laser beam direction using a Hammamatsu R928 photomultiplier (PM) tube and a cutoff filter set. However, the phosphorescence emission spectra were obtained by using a monochro-

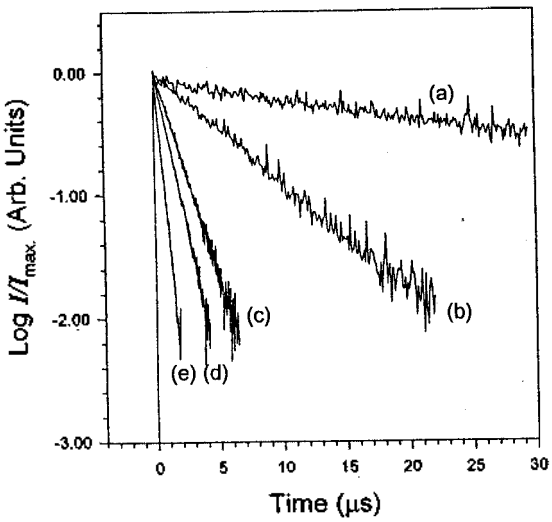

Figure 1. The phosphorescence time profiles from the $^3B_1$ state of SO_2 at several different pressures: (a) 1.5, (b) 10.1, (c) 52.0, (d) 100, and (e) 500 Torr.

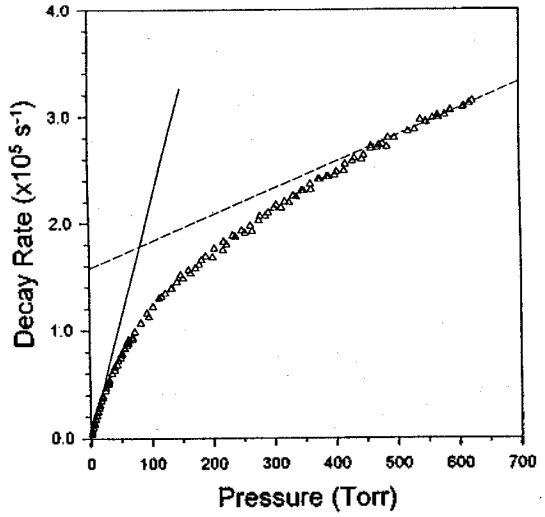

Figure 2. The pressure dependence of the phosphorescence decay rates of the $^3B_1$ state of SO_2 in the pure SO_2 at 26.0 ℃. The solid lines are the least square fitting lines for the low (≤5.0 Torr) and high (≥500 Torr) pressure data.

mator (Spex 500M) equipped with a holographic grating. The signal from the PM tube was fed to a digitizing oscilloscope (Tektronix TDS520) for the digitization and signal averaging and transferred to a laboratory computer for storage and analysis. Experiments were done in both static and slowly flowing (~0.5 mmoles/min) conditions but the decay rates at a given pressure were the same.

Results and Discussions

Pressure dependence of the phosphorescence decay rates. The phosphorescence from the $^3B_1$ state of SO_2 molecules following laser excitation exhibited a good single exponential decay behavior as shown in Figure 1 We have collected the time profiles at 26 ℃ and analyzed them to

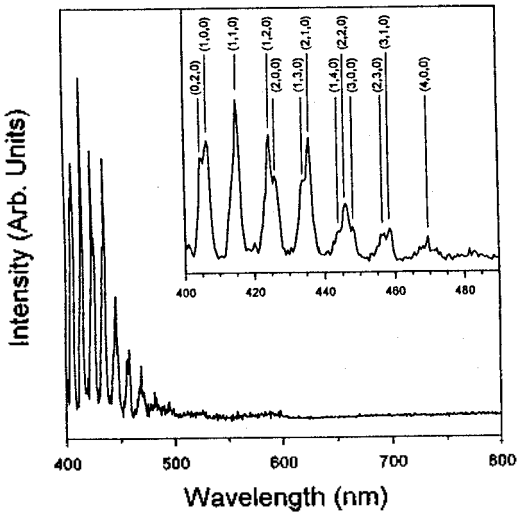

Figure 3. Phosphorescence emission spectrum taken from $^3B_1$ (0,1,0) excitation at 100.0 Torr of SO_2. The emissions were collected for 0-8.0 μs period following the laser excitation, which corresponds to about ten times of the phosphorescence decay rates at 100.0 Torr of SO_2.

obtain the phosphorescence decay rates. The pressure dependence of the phosphorescence decay rates is plotted in Figure 2, which shows basically the same features as those reported by other groups.[5~7,9] There appears two linear regions in Figure 2. The slope and intercept for the low pressure region are $(6.7\pm 0.2)\times 10^{-13}$ cm^{3}molecule^{-1}s^{-1} and (120 ± 40) s^{-1}, respectively. At the low pressure limit, $k_q[SO_2] \ll 1$, the third term of the right-hand side in Eq. (4) reduces to $k_q[SO_2]$. Therefore, the slope and intercept obtained from the low pressure data correspond to (k_q+k_c) and $1/\tau^0$, respectively, and they are in good agreement with the quenching and radiative decay rate constants of the $^3B_1$ state of SO_2 reported previously.[8] On the other hand, the slope and intercept in the high pressure region are $(8.7\pm 0.2)\times 10^{-14}$ cm^3 molecule^{-1} s^{-1} and $(1.6\pm 0.2)\times 10^6$ s^{-1}, respectively. When the pressure is high enough to fulfill $k_q[SO_2] \gg 1$, then the physical quenching term in Eq. (4) reduces to a constant. Thus the slope from the high pressure data corresponds to the chemical quenching rate constant (k_c) and the intercept is basically $1/\alpha$ since the contribution of radiative decay rate to the intercept is negligible.

Phosphorescence Emission Spectra and the Kinetic Model. Strickler and Ito[6] prepared indirectly the $^3B_1$ state of SO_2 by exciting the ground state molecules to the $^1A_2$ state at 315.6 nm and allowing collisional decay to the $^3B_1$ state. They investigated the plausible phosphorescence in the visible region for the $^3A_2 \rightarrow X^1A_1$ transitions. They were unable to observe any evidence of the $^3A_2 \rightarrow X^1A_1$ phosphorescence in the visible region. We have prepared the $^3B_1(0,0,0)$ and $^3B_1(0,1,0)$ molecules directly pumping the ground state SO_2 molecules at 388.3 and 382.5 nm, respectively, and investigated the emission spectra in the 400-800 nm region. A typical emission spectrum obtained from the $^3B_1(0,1,0)$ level excitation at 100.0 Torr of SO_2 is shown in Figure 3. The spectrum was taken by collecting emissions for 0-8 μs after the laser excitation. The observation period corresponds to

about ten times of the phosphorescence decay time of the $^3B_1$ state at 100.0 Torr. As shown in Figure 3, all the structured emission peaks appeared in the 400-500 nm region correspond to the $a^3B_1 \rightarrow X^1A_1$ vibronic transitions[10] and no new band was observed. This result agrees with that of Strickler and Ito.[5]

The kinetic model suggested by Strickler and Rudolph[5] is based on the Hiller and Saunders' theoretical calculations[11] and the experimental observations of the rotational line perturbation in the $^3B_1$ state by Brand *et al.*[10a] The kinetic model is based on the assumption of the strong coupling between the $^3B_1$ state and the near-lying $^3A_2$ state which is expected to have a radiative decay path to a lower-lying $^3B_2$ state. However, Avouris *et al.*[12] investigated those low-lying electronic states of SO_2 using the electron energy loss spectroscopy, and found that the $^3B_1$ state is the lowest triplet. Also, the recent more reliable theoretical calculations by Kamiya and Matsui[13] showed that the $^3A_2$ state located much higher in energy than the $^3B_1$ state. Another negative evidence for the location of the $^3A_2$ state is found from the recent vibrational relaxation studies in the $^3B_1$ state.[8] If the $^3A_2$ state were to be located in about 300 cm^{-1} above the $^3B_1(0,0,0)$ level, the interaction between the $^3B_1(0,1,0)$ level and $^3A_2$ state should be strong and affect on the equilibrium kinetics between the $^3B_1(0,0,0)$ and the $^3B_1(0,1,0)$ levels, because the energy gap between them is just about 50 cm^{-1}. However, the time profiles from the $^3B_1(0,0,0)$ and $^3B_1(0,1,0)$ levels obtained by exciting either the $^3B_1(0,0,0)$ or the $^3B_1(0,1,0)$ level were fitted well by the well-known three-level kinetic scheme[14] without considering other near-lying electronic state. Thus, the kinetic model is not appropriate to explain the pressure saturation of the phosphorescence decay rates of the $^3B_1$ state of SO_2.

Radiationless Transition Model. The pressure saturation effect of the phosphorescence decay rates of the $^3B_1$ state of SO_2 is qualitatively explained by the Freed's theory of collision-induced intersystem crossing (CIISC).[15] However, the pressure saturation of the $^3B_1$ state of SO_2 molecules was observed at much lower pressures than predicted by the Freed's theory of CIISC.

The radiationless transition model proposed by Strickler and Rudolph is based on the time-dependent perturbation theory.[16] They calculated the probability of the collisional intersystem crossing from the individual vibronic levels of the $^3B_1$ state to the nearly isoenergic, high-lying vibrational levels of the ground state. According to this model, the radiative decay and the chemical quenching terms remain the same as in Eq. (4), however, the physical quenching term is given by the following Eq. (5),[5,6]

$$\frac{2\pi\beta^2\rho Z}{\sqrt{4\beta^2+\hbar^2Z^2}} = \frac{\pi\beta\rho Z}{\sqrt{1+(\hbar^2Z^2/4\beta^2)}} = \frac{k_q[SO_2]}{\sqrt{1+\alpha^2k_q^2[SO_2]^2}} \quad (5)$$

where β is a coupling matrix element between the two states, ρ is the density of ground-state vibrational levels, Z is the average frequency of collisions giving rotational relaxation, $k_q=\pi\beta\rho Z/[SO_2]$ and $1/\alpha=2\pi\beta^2\rho/\hbar$ are the physical quenching rate constants at low- and high-pressure limits, respectively. The ρ can be obtained by direct count[17] of the vibrational energy levels of the ground state located near the low-lying vibrational levels of the $^3B_1$ state and the energies

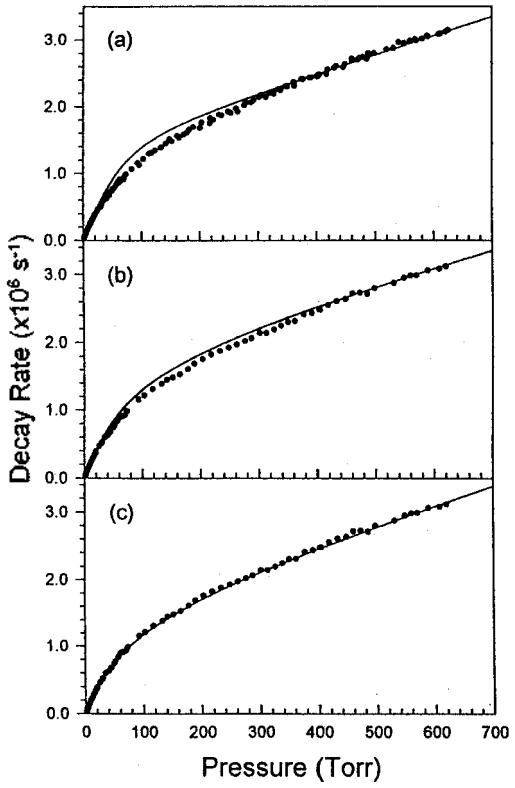

Figure 4. Comparison of the experimental (●—●) and calculated (—) pressure dependence of the phosphorescence decay rates. The parameters for the calculated data in (a), (b), and (c) are given by Eqs. 6, 10 and 11, respectively.

of the ground state vibrational levels are calculated using the known molecular constants.[18] Since the $1/\alpha$ obtained from the experiment is $(1.6\pm 0.2)\times10^6$ s^{-1}, and since the obtained from the direct counting method[17] is 0.63-0.68 $/cm^{-1}$, the magnitude of the coupling constant, β, is $(1.3\text{-}1.4)\times10^{-3}$ cm^{-1} on the average. This value of the coupling constant is in good agreement with that of Strickler and Rudolph.[5] Using the β obtained from the high pressure data, the Z can be estimated to be 2.1×10^{-10} $[SO_2]$ s^{-1} from the difference between the magnitude of the slopes for the low- and high-pressure regions. Because the slope from the low-pressure data corresponds to the sum of physical and chemical quenching rate constants while that from the high-pressure region represents the chemical quenching rate constant.

We have investigated the pressure dependence of the decay rates over the whole pressure range. The decay rates at various pressures are calculated from the Eqs. (4) and (5) using the following values of β, ρ and Z assuming that the coupling matrix elements are the same for all of the interacting vibrational levels.

$$\begin{aligned}&\beta=1.35\times10^{-3}\ cm^{-1}\\&\rho=0.64\ /cm^{-1}\\&Z=2.1\times10^{-10}\ [SO_2]\ s^{-1}\end{aligned} \quad (6)$$

However, the pressure dependence of the phosphorescence decay rates in the 30-350 Torr range cannot be fitted well as shown in Figure 4(a). The misfit in the medium pressure region could be the consequence of ignoring the variation

of β for the different vibrational levels. Thus, we have looked for the improvement of fitting by assigning different coupling constants for those low-lying vibrational levels of the $^3B_1$ state, since substantial amounts of the molecules are distributed in the (0,1,0) and (0,2,0) levels due to the relatively small fundamental vibrational frequency of the bending mode (361 cm^{-1}). Since the vibrational relaxation rates are much larger than the quenching rate constants,[8] the vibration population ratios among the vibrational levels of the $^3B_1$ state should be Boltzmann. When the coupling matrix elements are not the same for the different vibrational levels, the physical quenching term given by Eq. (5) can be rewritten as Eq. (7),

$$\pi Z\left\{\frac{f_0\beta_0\rho_0}{\sqrt{1+(\hbar Z^2/4\beta_0^2)}}+\frac{f_1\beta_1\rho_1}{\sqrt{1+(\hbar Z^2/4\beta_1^2)}}+\frac{f_2\beta_2\rho_2}{\sqrt{1+(\hbar Z^2/4\beta_2^2)}}\right\}$$

$$=\left\{\frac{k_{q0}f_0}{\sqrt{1+\alpha_0^2k_{q0}^2[SO_2]^2}}+\frac{k_{q1}f_1}{\sqrt{1+\alpha_1^2k_{q1}^2[SO_2]^2}}+\frac{k_{q2}f_2}{\sqrt{1+\alpha_2^2k_{q2}^2[SO_2]^2}}\right\}\times[SO_2] \quad (7)$$

where the subscripts (0, 1 and 2) are used to represent the (0,0,0), (0,1,0) and (0,2,0) levels, respectively, and f is the fractions of the molecules in each vibrational level of the $^3B_1$ state. At the low- and high-pressure limits, the physical quenching rate constants are given by Eq. (8).

$$\pi(f_0\beta_0\rho_0+f_1\beta_1\rho_1+f_2\beta_2\rho_2)\frac{Z}{[SO_2]}=5.8\times10^{-13}\ cm^3\ molecules^{-1}s^{-1} \quad (8a)$$

$$\frac{f_0}{\alpha_0}+\frac{f_1}{\alpha_1}+\frac{f_2}{\alpha_2}=\frac{2\pi}{\hbar}(f_0\beta_0^2\rho_0+f_1\beta_1^2\rho_1+f_2\beta_2^2\rho_2)=1.6\times10^6\ s^{-1} \quad (8b)$$

The population ratios among the (0,0,0), (0,1,0), and (0,2,0) levels of the $^3B_1$ state in equilibrium are 0.829 : 0.145 : 0.026 at 26 ℃, and the density of the ground state vibrational levels in the vicinity of these vibrational levels of the $^3B_1$ state are 0.63, 0.66, and 0.68 /cm^{-1}, respectively.[17] Substituting appropriate numerical values into the Eq. (8) and dividing both side by $\pi f_0\rho_0$ and $2\pi f_0\rho_0/\hbar$, respectively, Eq. (9) is obtained.

$$(\beta_0+0.1832\beta_1+0.03385\beta_2)\frac{Z}{[SO_2]}=3.535\times10^{-13}\ cm^3\ molecule^{-1}s^{-1} \quad (9a)$$

$$\beta_0^2+0.1832\beta_1^2+0.03385\beta_2^2=2.589\times10^{-6}\ cm^{-2} \quad (9b)$$

Eq. (9) are undetermined coupled equations, so they have numerous solutions. If we assume an equal contribution (33 %) from each vibrational level, we obtain the following set of coupling constants and Z.

$$\beta_0=9.29\times10^{-4}\ cm^{-1}$$
$$\beta_1=2.17\times10^{-3}\ cm^{-1}$$
$$\beta_2=9.29\times10^{-3}\ cm^{-1}$$
$$Z=2.36\times10^{-10}\ [SO_2]\ s^{-1} \quad (10)$$

The curve fitting using the above coupling constants also showed substantial deviations in the medium pressure region as plotted in Figure 4(b). However, it was found that the curve fitting could be improved by adjusting the ratios of contribution from each vibrational level to the intersystem crossing. When the contributions from the (0,0,0), (0,1,0) and (0,2,0) level were assumed to be in the range of 20-25%, 30-35% and 45-50% of the total physical quenching rate at high-pressure limits, respectively, the whole range of the experimental curve could be fitted well as plotted in Figure 4(c). Thus, we obtain the following constants for β_f and Z assuming that the contributions from (0,0,0), (0,1,0) and (0,2,0) levels are 20, 35, and 45%, respectively.

$$\beta_0=7.2\times10^{-4}\ cm^{-1}$$
$$\beta_1=2.2\times10^{-3}\ cm^{-1}$$
$$\beta_2=5.9\times10^{-3}\ cm^{-1}$$
$$Z=2.7\times10^{-10}\ [SO_2]\ s^{-1} \quad (11)$$

The Z value obtained in this work seemed to be about 20% larger than the gas kinetic rate constant, 2.3×10^{-10} $cm^3molecule^{-1}s^{-1}$, calculated from the van der Waals radius (4.1 Å) of the ground state SO_2 molecules. When the ground state SO_2 molecule is excited to the $^3B_1$ state, the geometry of the molecule changes: the bond length of the molecule increases from 1.432 Å to 1.493 Å and the bond angle also increases from 119.5° to 126.2°.[10a] Thus the wan der Waals radius of the $^3B_1$ state should be larger than that of the ground state, which might result in the larger Z value.

We did not investigate the temperature dependence of the physical quenching rate at high-pressure limits in this work. However, the saturated physical quenching rate should have a component of temperature dependence, because the relative populations in Eq. (7) change as the temperature changes. The saturated quenching rate, $1/\alpha_s$, is given by Eq. (12),

$$\frac{1}{\alpha_s}=\frac{f_0}{\alpha_0}+\frac{f_1}{\alpha_1}+\frac{f_2}{\alpha_2}=\frac{2\pi}{\hbar}(f_0\beta_0^2\rho_0+f_1\beta_1^2\rho_1+f_2\beta_2^2\rho_2)$$

$$=\frac{2\pi}{\hbar Q}\left[\beta_0^2\rho_0\exp\left(-\frac{\varepsilon_0}{kT}\right)+\beta_1^2\rho_1\exp\left(\frac{\varepsilon_1}{kT}\right)+\beta_2^2\rho_2\exp\left(\frac{\varepsilon_2}{kT}\right)\right] \quad (12)$$

where Q is the vibrational partition function of the $^3B_1$ state. Although the above Eq. (12) can not be reduced to the simple Arrhenius form, the temperature dependence of $1/\alpha_s$ can be examined by a numerical method. The temperature dependence of $1/\alpha_s$ calculated from Eq. (12), using the β_f given in Eq. (11) and energy level densities obtained by direct counting method, is given in Table 1. When the ln $(1/\alpha_s)$ *vs.* $1/T$ is plotted as shown in Figure 5, the slope corresponds to the apparent activation energy of ~420 cm^{-1}. This apparent activation energy is substantially smaller compared with the (700± 100) cm^{-1} reported by Strickler and Ito.[6] However, a closer look at the experimental data of Strickler and Ito

Table 1. Temperature dependence of the calculated $1/\alpha_s$

Temp. (℃)	$1/T$ (10^{-3} K^{-1})	f_0	f_1	f_2	$1/\alpha_s$ (10^6 s^{-1})	ln $(1/\alpha_{calc})$
26.0	3.342	0.829	0.145	0.026	1.597	14.284
35.0	3.245	0.820	0.151	0.029	1.700	14.346
45.0	3.143	0.810	0.158	0.032	1.807	14.407
55.0	3.047	0.801	0.164	0.035	1.910	14.463
65.0	2.957	0.792	0.170	0.038	2.014	14.516

(a) $\frac{1}{\alpha_s}=\frac{2\pi}{\hbar}(f_0\beta_0^2\rho_0+f_1\beta_1^2\rho_1+f_2\beta_2^2\beta_2)$

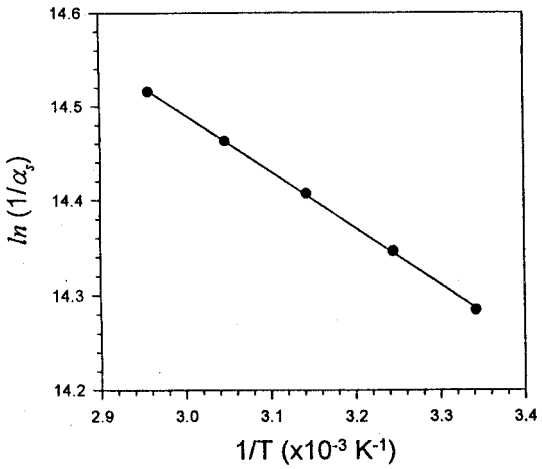

Figure 5. Temperature dependence of $1/\alpha_s$ calculated using the constants given by Eq. (11). The apparent activation energy obtained from the slope is ~420 cm^{-1}.

showed that they might make an overestimation of the activation energy by including those data in the medium pressure region to obtain $1/\alpha$. When the decay rates in the medium pressure region are included, the evaluated $1/\alpha$ should be smaller than the saturated quenching rate. When the $1/\alpha$ is reestimated from the Strickler and Ito's data for $p \geq 500$ Torr, we obtain (500 ± 100) cm^{-1} as the apparent activation energy from the temperature dependence of the $1/\alpha$. This value is in fair agreement with the one obtained from Figure 5, and supports the model suggested in this work.

Conclusion

We have reinvestigated the pressure saturation effect on the phosphorescence decay rates of the $^3B_1$ state of SO_2 by the laser induced phosphorescence method. It is shown that the pressure dependence of the phosphorescence decay rates of the $^3B_1$ state measured in this work can be fitted well by the Strickler and Rudolph's radiationless transition model assigning different magnitude of the coupling matrix element to the different vibrational levels of the $^3B_1$ state. The temperature dependence of the saturated physical quenching rate can also be explained by the larger coupling matrix elements for vibrationally excited levels since the relative populations in each vibrational level change as the temperature changes. It is shown that the physical quenching of the $^3B_1$ state of SO_2 should occur primarily through the vibrationally excited levels, and the (0,2,0) level is the most important channel for the physical quenching process.

Acknowledgment. This work is financially supported in part by Korea Science and Engineering Foundation through the Center for Molecular Science at KAIST and in part by the Basic Science Research Institute Program (BSRI-95-3438), Ministry of Education.

Reference

1. Heicklen, J.; Kelly, N.; Partymiller, K. *Rev. Chem. Intermediates* **1980**, *3*, 315.
2. Heicklen, J. *Atmospheric Chemistry*; Academic: New York, 1976.
3. Chung, K.; Calvert, J. G.; Bottenheim, J. W. *Int. J. Chem. Kinet.* **1975**, *7*, 161.
4. (a) Otsuka, K.; Calvert, J. G. *J. Am. Chem. Soc.* **1971**, *93*, 2581. (b) Sidebottom, H. W.; Badcock, C. C.; Calvert, J. G.; Reinhardt, G. W.; Rabe, B. R.; Damon, E. K. *J. Am. Chem. Soc.* **1971**, *93*, 2587.
5. Strickler, S. J.; Rudolph, R. N. *J. Am. Chem. Soc.* **1978**, *100*, 3326.
6. Strickler, S. J.; Ito, R. D. *J. Phys. Chem.* **1985**, *89*, 2366.
7. Su, F.; Wampler, F. B.; Bottenheim, J. W.; Thorsell, D. L.; Calvert, J. G.; Damon, E. K. *Chem. Phys. Lett.* **1977**, *51*, 150.
8. Bae, S. C.; Lee, K.; Kim, G. H.; Ku, J. K. *J. Chem. Phys.* **1995**, *102*, 1665.
9. (a) Wampler, F. B.; Oldenborg, R. C.; Rice, W. W.; Karl, R. R. Jr. *J. Chem. Phys.* **1978**, *69*, 2569. (b) Wampler, F. B.; Oldenborg, R. C.; Rice, W. W. *Int. J. Chem. Kinet.* **1979**, *11*, 125.
10. (a) Brand, J. C. D.; Jones, V. T.; Di Lauro, C. *J. Mol. Spectrosc.* **1973**, *45*, 404. (b) Hochstrasser, R. M.; Marchetti, A. P. *J. Mol. Spectrosc.* **1970**, *35*, 335. (c) Carter, S.; Mills, I. M.; Murrell, J. N.; Varandas, A. J. C. *Mol. Phys.* **1982**, *45*, 1053.
11. Hiller, I. H.; Saunders, V. R. *Mol. Phys.* **1971**, *22*, 193.
12. Avouris, Ph.; Demuth, J. E.; Schmeisser, D.; Colson, S. C. *J. Chem. Phys.* **1982**, *77*, 1062.
13. Kamiya, K.; Matsui, H. *Bull. Chem. Soc. Jpn.* **1991**, *64*, 2792.
14. Yardley, J. T. *Introduction to Molecular Energy Transfer*; Academic: New York, 1980.
15. (a) Freed, K. F. *Adv. Chem. Phys.* **1982**, *47-II*, 291. (b) Freed, K. F. *Acc. Chem. Res.* **1978**, *11*, 74.
16. Robinson, G. W.; Frosch, R. P. *J. Chem. Phys.* **1962**, *37*, 1962.
17. (a) Current, J. H.; Rabinovitch, B. S. *J. Chem. Phys.* **1963**, *38*, 783. (b) Stein, S. E.; Rabinovitch, B. S. *J. Chem. Phys.* **1973**, *58*, 2438.
18. Yamanouchi, K.; Takeuchi, S.; Tsuchiya, S. *J. Chem. Phys.* **1990**, *92*, 4044.